

---

## ANALYSIS OF GRID INTEGRATED DOUBLY FED INDUCTION GENERATOR BUILT WIND TURBINE WITH ENHANCED FAULT RIDE THROUGH CAPABILITY: A DYNAMIC AND TRANSIENT PERSPECTIVE

Md Sajid Hossain\*<sup>1</sup>

\*<sup>1</sup>Assistant Professor, Department Of Electrical & Electronics Engineering, American International University – Bangladesh (AIUB), Dhaka, Bangladesh.

DOI : <https://www.doi.org/10.56726/IRJMETS59986>

---

### ABSTRACT

The integration of renewable energy sources, particularly wind power into the electrical grid presents challenges in maintaining grid stability. This research paper focuses on enhancing the Low-Voltage Ride-Through (LVRT) capability of a Doubly-Fed Induction Generator (DFIG) wind turbine connected to the grid. LVRT is crucial for ensuring that wind turbines remain operational during voltage dips or faults, contributing to overall grid reliability. The study emphasizes the importance of complying with grid codes, which dictate specific requirements for voltage recovery after a fault event. To evaluate the LVRT performance of the DFIG wind turbine system, both dynamic and transient analyses are conducted. The dynamic analysis examines the system's behavior over extended periods under varying wind conditions, while the transient analysis focuses on short-duration events like faults. A critical aspect of this research is the optimization of Proportional-Integral (PI) controllers. These controllers play a vital role in regulating the reactive power injected into the grid during disturbances, aiding in voltage recovery and stability. The effectiveness of the PI control strategy is evaluated using the PSCAD/EMTDC® simulation software, a widely recognized tool for power system modeling and analysis. The simulation results demonstrate the positive impact of the optimized PI controllers on LVRT capability. By strategically controlling reactive power injection, the system can effectively mitigate voltage dips and ensure compliance with grid code requirements. This research contributes to the ongoing efforts to integrate wind energy into the power grid while maintaining its stability and reliability.

**Keywords:** Augmentation, Grid Integration, LVRT, Wind Power, Dynamic Analysis, Transient Analysis.

---

### I. INTRODUCTION

The increasing integration of wind power into electrical grids necessitates robust solutions to ensure stability and reliability. Low Voltage Ride Through (LVRT) capability is crucial for the seamless integration of wind power into the grid, as it allows wind turbines to remain connected and operational during voltage dips. Voltage dips, often caused by faults or sudden changes in load, can pose significant challenges to the stability of the electrical grid. Without effective LVRT mechanisms, wind turbines may disconnect during these events, exacerbating grid instability.

To enhance LVRT performance, various augmentation techniques are employed, which are vital for maintaining grid stability. These techniques include advanced control strategies, energy storage systems and reactive power support, all designed to improve the resilience of wind turbines during transient disturbances. Implementing these augmentation measures ensures that wind turbines can withstand voltage drops and continue to contribute to the grid, thereby enhancing overall system reliability.

Comprehensive dynamic and transient analyses are essential in assessing and optimizing these techniques. Dynamic analysis involves examining the behavior of wind power systems under normal and disturbed operating conditions over time. This analysis helps in understanding how wind turbines respond to changes in wind speed, grid faults and other disturbances. Transient analysis, on the other hand, focuses on the system's immediate response to sudden changes, such as faults or switching operations, providing insights into the short-term stability and performance of the system.

Large scale integration of wind turbine into the power grid demands strict adherence to grid codes, particularly under dynamic grid conditions. One critical aspect of these regulations is the Low Voltage Ride Through (LVRT) capability. LVRT requires wind turbines to remain connected and operational during voltage dips, ensuring rapid voltage recovery. Specifically, wind turbines must restore 90% of the pre-fault voltage within 1.5 seconds

and contribute reactive power during disturbances to support grid voltage stability [1,2]. Researchers have explored various control strategies to enhance Low-Voltage Ride-Through (LVRT) or Fault-Ride-Through (FRT) capabilities in these systems.

One approach involves modifying Proportional-Integral (PI) controllers using optimization algorithms like the Elephant Herding Algorithm (EHA). This method has shown promise in improving voltage regulation and grid stability compared to other optimization techniques like Cuckoo Search Optimization (CSO) and Particle Swarm Optimization (PSO) [3]. Another strategy focuses on combining fixed and variable speed wind turbine technologies to enhance LVRT. This hybrid approach aims to overcome the limitations of fixed-speed turbines in providing reactive power support during faults, while also addressing the cost concerns associated with variable speed turbines. A fuzzy logic-based controller is employed to optimize the system's response to disturbances [4].

In the context of photovoltaic (PV) systems, researchers have proposed using the Salp Swarm Algorithm (SSA) to optimize controller parameters. This approach focuses on improving settling time, overshoot/undershoot and steady-state error in voltage regulation, thereby enhancing LVRT criteria [5]. For offshore wind farms, a hybrid optimization method combining Cuckoo Search Optimization (CSO) and Gray Wolf Optimizer (GWO) has been applied to design and tune PI controllers, aiming to improve overall performance [6]. Coordinated control strategies have also been explored to address both LVRT and grid frequency stability. These strategies often involve battery storage systems equipped with modified PI controllers and static-based controllers. By adjusting active and reactive power during transient and dynamic periods, these systems can improve both frequency and LVRT response respectively [7].

While advanced control schemes offer potential benefits, their complexity and reliance on developer expertise can be a limitation. To address this, some researchers have employed the Taguchi method, a well-established optimization technique, to refine PI controllers in a cascaded configuration. This approach simplifies the design process and reduces the dependence on extensive training [8]. Recent studies have explored the use of optimization algorithms to enhance PI controllers. The Elephant Herding Algorithm (EHA) has shown significant promise in this regard, offering superior voltage regulation and grid stability compared to traditional algorithms like Cuckoo Search Optimization (CSO) and Particle Swarm Optimization (PSO) [9]. EHA optimizes the control parameters more effectively, ensuring better performance under fault conditions.

Combining fixed and variable speed wind turbine technologies has been proposed to enhance LVRT capabilities. This hybrid approach addresses the limitations of fixed-speed turbines in providing reactive power during faults while also mitigating the cost implications of variable speed turbines. A fuzzy logic-based controller is used to optimize the system's response to disturbances, improving overall stability and performance [10]. For photovoltaic (PV) systems, the SSA has been employed to optimize controller parameters. This algorithm focuses on improving the settling time, overshoot/undershoot, and steady-state error in voltage regulation, thereby enhancing LVRT criteria [11].

A novel hybrid optimization method combining Cuckoo Search Optimization (CSO) and Gray Wolf Optimizer (GWO) has been used to design and tune PI controllers for offshore wind farms. This method aims to improve overall system performance by leveraging the strengths of both algorithms. Coordinated control strategies often involve the integration of battery storage systems with modified PI controllers and static-based controllers. These systems adjust active and reactive power during transient and dynamic periods, enhancing both grid frequency and voltage stability [12]. By providing a buffer during voltage sags, these systems can maintain grid stability more effectively. Voltage stability analysis using FACTS devices, such as STATCOMs and SVCs, has been extensively studied. STATCOMs have shown superior performance in improving voltage stability by providing dynamic reactive power compensation during faults [13]. To address the complexity of advanced control schemes, researchers have employed the Taguchi method to refine PI controllers in a cascaded configuration. This optimization technique simplifies the design process, reducing the need for extensive expertise and training while maintaining effective LVRT capabilities [14].

With the rapid growth in renewable energy, particularly wind power, maintaining grid stability and reliability has become increasingly challenging. As the penetration of renewable sources escalates, grid regulations have evolved to ensure that these sources do not compromise the stability of the power network. Historically, grid

codes were less stringent due to the minimal impact of renewable energy [15]. However, the surge in renewable energy integration has necessitated more rigorous standards to uphold grid stability.

This paper delves into the dynamic and transient responses of wind power systems with a focus on LVRT augmentation. By conducting detailed simulations and practical assessments, we aim to provide a thorough understanding of how different augmentation techniques impact the grid integration of wind power. The insights gained from this study will contribute to the development of more effective strategies for enhancing LVRT capability, ultimately leading to more resilient and stable electrical grids with higher penetration of renewable energy sources

## II. METHODOLOGY

Wind turbines capture energy from the wind and their power output fluctuates due to changes in wind speed. The power generated by a wind turbine can be calculated using a very well-known mathematical equation [16]

$$P_w = \frac{1}{2} \rho \pi R^2 U_w^3 C_p(\lambda, \beta) \tag{1}$$

Figure 1 illustrates the pitch angle controller used for a DFIG to ensure that the generator's output power remains at or below its rated level. The pitch angle controller continuously monitors the output power of the DFIG. If the output power exceeds the rated level, the controller adjusts the pitch angle,  $\beta^*$  to reduce the power captured by the turbine blades. The PI controller ensures a calculated and smooth adjustment by considering both the current error and the accumulated past errors. The first-order lag filter ensures these adjustments are gradual to maintain the system stability and prevent mechanical wear-off.

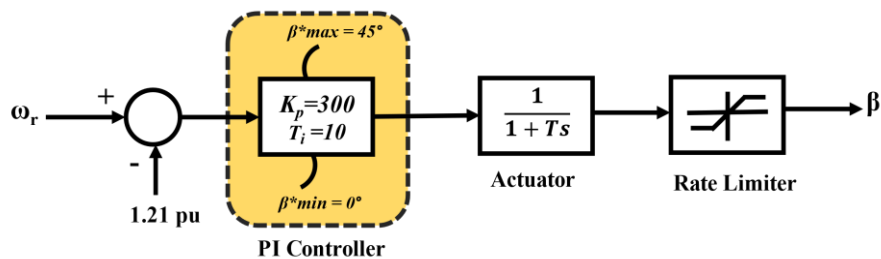


**Figure 1:** Pitch Angle Controller for DFIG.

By maintaining the pitch angle within specified limits and ensuring smooth transitions, the controller effectively keeps the generator's output power at or below the rated level, protecting the generator from overloading and ensuring efficient operation.

Figure 2 shows a comprehensive model of a DFIG wind turbine system. This system includes several key parts:

- A model that simulates how the wind interacts with the turbine blades.
- A special type of generator called a Wound-Rotor Induction Generator (WRIG) that converts wind energy into electricity.
- A converter that helps control the flow of electricity between the generator and the grid.
- A circuit that protects the system and ensures stable power delivery.
- Converters on both the rotor side (RSC) and the grid side (GSC) to manage the electrical power.

The analysis uses a built-in model of the WRIG. The stator of the WRIG is directly connected to the power grid, while the rotor is connected through a converter that handles about 30% of the total power. The wind drives the WRIG, which converts wind energy into electrical energy. The WRIG also determines the speed and position of the rotor. A pitch angle controller adjusts the angle of the blades to control the power output when the turbine spins too fast. Finally, a transformer connects the GSC to the grid system.

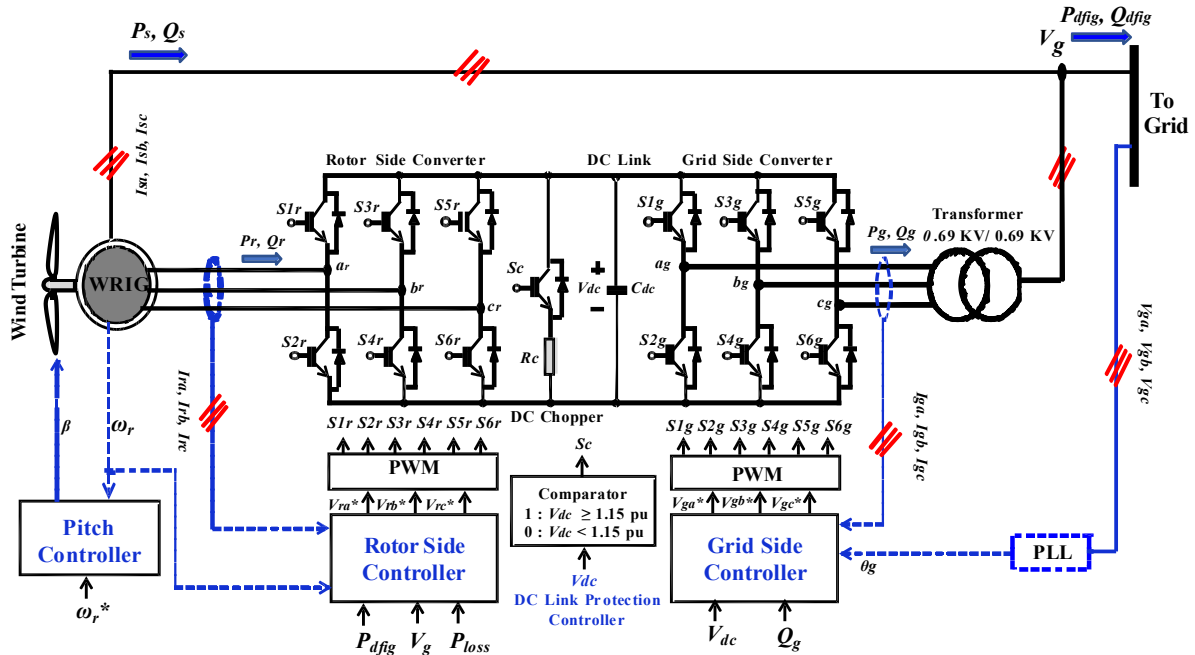


Figure 2: In-depth Layout of DFIG Configuration

Figure 3 depicts the implementation of four Proportional-Integral (PI) controllers in a Rotor Side Converter (RSC) used to manage different error signals in a grid-connected system. The idea is about controlling the active and reactive power sent to the grid by adjusting the rotor currents on the "q" and "d" axes. The PI controllers process error signals related to the rotor currents on the "q" (quadrature) and "d" (direct) axes. These error signals are deviations from the desired reference values for these currents. The reference grid voltage is maintained at 1.0 per unit (pu) to comply with grid code standards, ensuring stable and reliable operation of the grid-connected system.

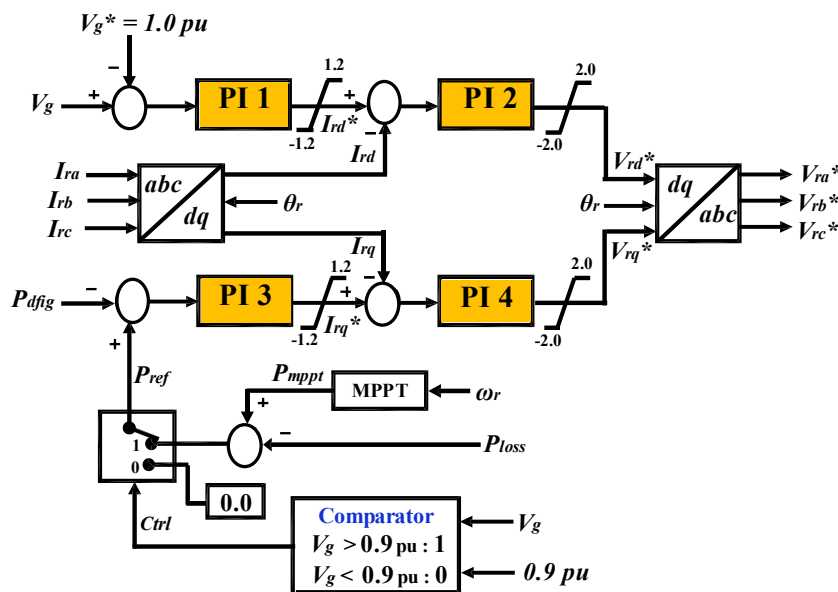


Figure 3: Controller on the Rotor Side of DFIG.

Figure 4 illustrates the implementation of four Proportional-Integral (PI) controllers in the Grid Side Converter (GSC) to manage different error signals. Four PI controllers are used in the GSC to manage error signals related to the control of DC link voltage and reactive power. Each controller handles specific error signals to ensure the system meets the desired performance criteria. The GSC needs to control two main parameters: the reactive power (kept at zero) and the DC link voltage (maintained at 1.0 per unit (pu)). These parameters are crucial for

complying with grid code standards and ensuring efficient operation [17], [18]. Maintaining the DC link voltage at 1.0 pu and keeping the reactive power at zero ensures that the GSC operates within the required standards set by the grid code. This compliance is critical for grid stability and reliable grid operations.

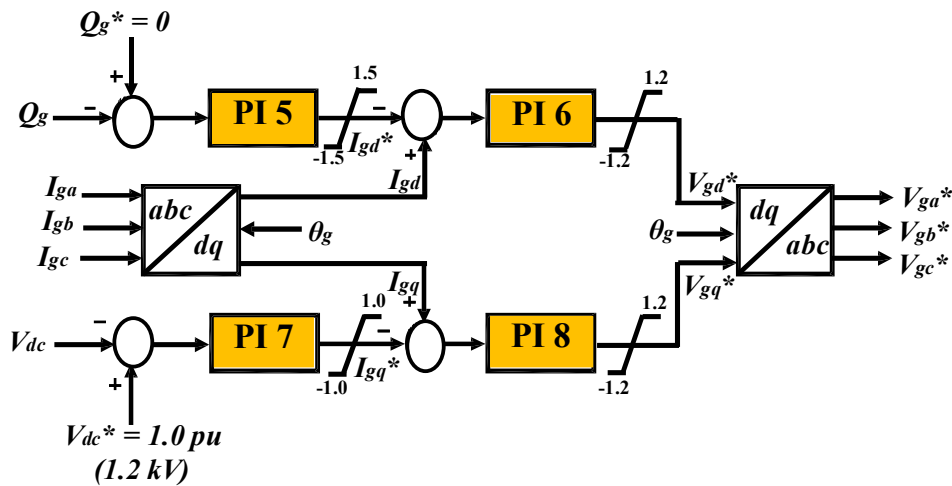


Figure 4: Controller on the Grid Side of DFIG.

Through optimization, the best values for the eight PI controllers were determined. These values were tested in various situations and the optimal settings are shown in Table 1. Limits are set on the PI controllers to make sure they work in realistic situations. This helps ensure that the right amount of reactive power is sent to the power grid, which is important for maintaining stable voltage during both short-term and long-term events [19].

Table 1. Optimized Parameters for Eight PI Controllers at RSC and GSC

PI Controllers	Controller Location	K <sub>P</sub>	K <sub>I</sub>
Proportional Plus Integral Controller 1	Rotor Side	1	8.7
Proportional Plus Integral Controller 2		0.79	8.8
Proportional Plus Integral Controller 3		1.2	13
Proportional Plus Integral Controller 4		0.03	0.05
Proportional Plus Integral Controller 5	Grid Side	1	9.9
Proportional Plus Integral Controller 6		0.89	8.2
Proportional Plus Integral Controller 7		1.1	11
Proportional Plus Integral Controller 8		0.02	0.07

### III. RESULTS AND ANALYSIS

#### Power System Model

Figure 5 shows a simplified diagram of the power system used in this study. A 20 MVA DFIG wind turbine is connected to a large power grid (represented as an infinite bus) through a transformer that increases the voltage from 0.69 kV to 6.6 kV. The connection also includes a short double transmission line with circuit breakers on each line. These circuit breakers can disconnect the wind turbine from the grid if there's a problem, like a fault or disturbance. Figure 5 also shows the resistance and inductance of the transmission lines. The system works at a standard frequency of 50 Hz and a base power of 100 MVA.

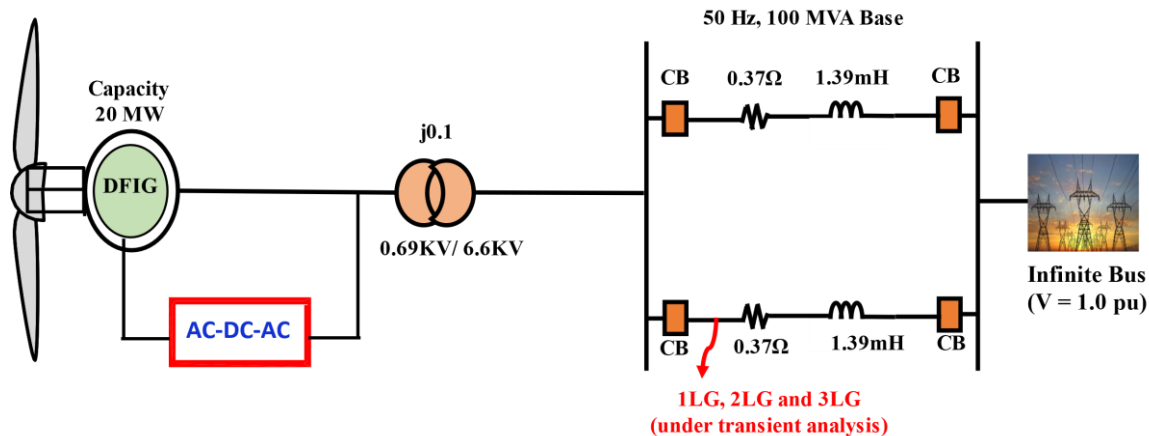


**Figure 5:** A Simplified Diagram of the Power System Model

The wind turbine drives the DFIG, which is capable of generating up to 20 MVA of power. The DFIG allows for variable speed operation and efficient energy capture from varying wind speeds. The DFIG is connected to an AC-DC-AC converter, enabling it to convert the generated power to a suitable form for grid integration. This converter consists of a rectifier (AC to DC) and an inverter (DC to AC), facilitating control over the power output. The power from the DFIG is stepped up by a transformer from 0.69 kV (the typical output voltage of a DFIG) to 6.6 kV, which is more suitable for transmission over the grid.

It also includes a short double transmission line segment. This segment represents the lines through which the generated power is transmitted to the grid. The resistance and inductance of these transmission lines are shown, which affect the power flow and stability of the system. Circuit breakers are installed on each of the transmission lines. These breakers can disconnect the wind turbine from the grid in case of faults or disturbances, protecting the system and enhancing reliability. The large power grid is represented as an infinite bus, which implies it has a constant voltage and frequency, unaffected by the power generated by the wind turbine. This is a standard assumption for large grids to simplify analysis.

The diagram indicates that transient analysis under various fault conditions was performed. This helps in understanding how the system responds to different types of electrical faults. The system operates at a standard frequency of 50 Hz, typical for many regions around the world. A base power of 100 MVA is used for per-unit system calculations, a common approach in power system analysis to simplify comparisons and calculations.

**Dynamic Stability Performance Analysis**

To analyze how the system performs under real-world conditions, we used real wind speed data [20] collected from Hokkaido Island in Japan, as presented in Figure 6. We used the same power system model from Figure 5 for this analysis. The dynamic analysis considered a long period of 300 seconds and included the fluctuating wind speed. Figure 6 shows how the wind speed varied between 8.5 m/s and 12.9 m/s during this time.

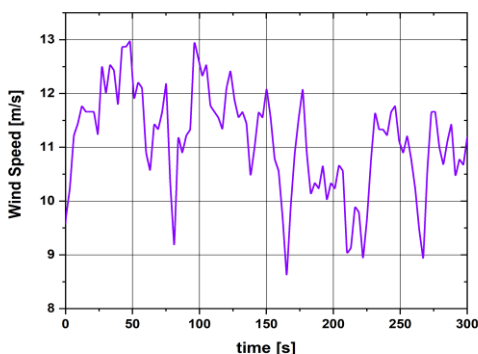


**Figure 6:** Data on Fluctuating Wind Speed.

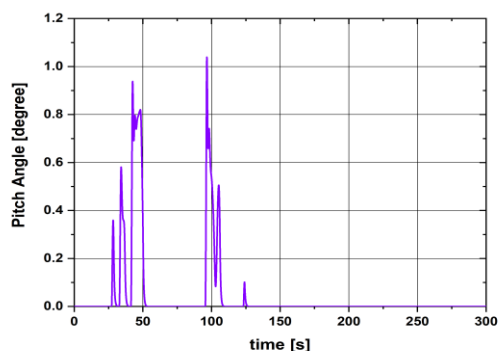


**Figure 7:** Response of Pitch Angle

In this study, we assume the rated wind speed for the DFIG wind turbine is 12.5 meters per second. Figure 7 shows how the pitch angle (the angle of the turbine blades) changes. When the wind speed goes above this rated speed (as seen in Figure 7), a controller automatically adjusts the blade angle to keep the turbine's power output under control. Pitch control is activated to prevent overloading the turbine during high wind speeds and to maximize energy capture during lower wind speeds.

The active power generated by the DFIG wind turbine fluctuates due to changes in wind speed. Since wind speed isn't constant, the power output varies accordingly. The maximum power output of the DFIG is close to 20 MW, which corresponds to 1.0 per unit (pu) when the wind speed reaches its ideal value of 12.5 m/s. The graph in Figure 8 shows that the active power occasionally peaks at around 20 MW, indicating times when the wind speed is optimal. Over a 300-second period, the active power output shows significant fluctuations. These fluctuations reflect the natural variability in wind speed and demonstrate how the DFIG responds to these changes. The power output ranges from 8 MW to nearly 20 MW.

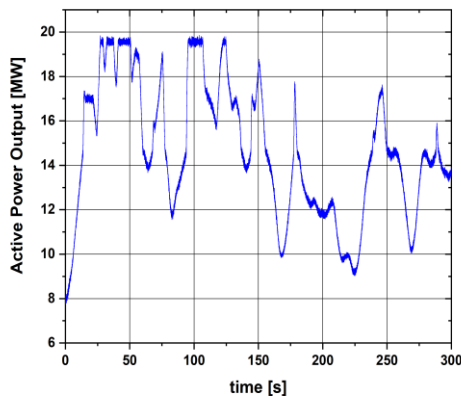


Figure 8: MW Output of Active Power

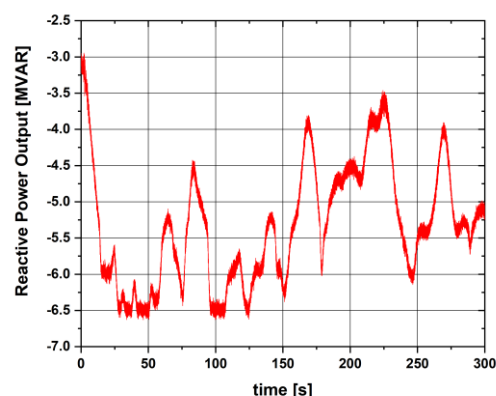


Figure 9: MVAR Output of Reactive Power

Figure 9 shows the reactive power output in megavolt-amperes reactive (MVAR). Reactive power is essential for maintaining voltage levels and ensuring efficient operation of the power system. Similar to active power, the reactive power output also fluctuates over time. This variation is influenced by changes in wind speed and the corresponding adjustments in the DFIG system to maintain stable operation. The graph indicates that the reactive power output varies between approximately -6.6 MVAR to -3.1 MVAR over the 300-second period. Negative values indicate that the DFIG is absorbing reactive power from the grid, which is common in wind turbines to help regulate voltage levels.

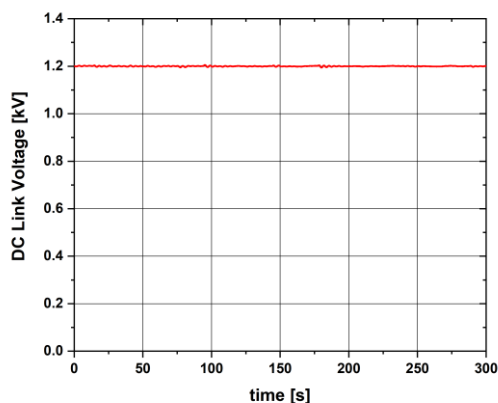


Figure 10: Response of Terminal Voltage

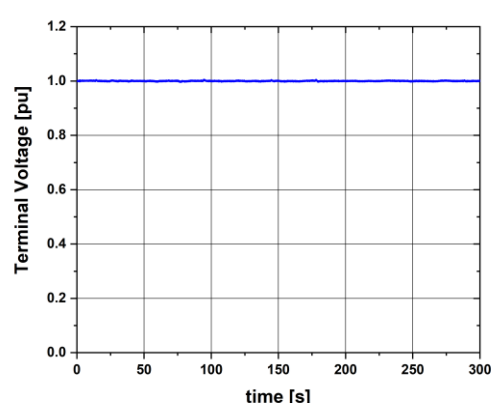


Figure 11: DC Link voltage feedback

Figure 10 shows that the terminal voltage stays steady at 1.0 pu (per unit), which means the adjusted PI controllers are doing a good job of managing the changes in line voltage over the studied period. Figure 11 shows that the DC link voltage of the DFIG also stays mostly constant. Even though the wind speed changes a

lot, the DC link voltage only changes a little. This shows that the system can maintain a stable voltage even when the wind speed varies.

**Transient Stability Performance Analysis**

Transient analysis focuses on how the system behaves over a short period. In this study, we simulated the system for 10 seconds to see how it reacts to different types of faults, including single-line-to-ground (1LG), double-line-to-ground (2LG), and the most severe type, a three-line-to-ground (3LG) fault. This helps us understand how well the adjusted PI controllers work and how robust the power system model is under these challenging conditions.

As shown in Figure 12, a fault was introduced at 1.1 seconds on one of the transmission lines (Figure 5). This fault lasted for 0.1 seconds, and after 1.2 seconds, the circuit breakers on that line opened to disconnect it from the rest of the power system. The circuit breakers were then closed again at 2.0 seconds, assuming the fault had been resolved. During this test, the wind speed was kept constant at the rated value of 12.5 m/s, as wind speed doesn't change much over short periods (10 seconds).

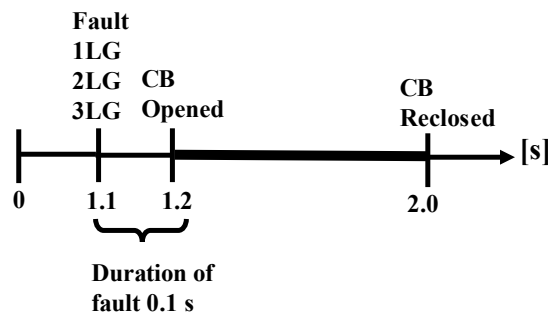


**Figure 12:** Transient Analysis Under Fault Condition

Figure 13 and Figure 14 illustrate the transient responses of a wind turbine system under different fault conditions: three-line-to-ground (3LG), two-line-to-ground (2LG), and single-line-to-ground (1LG) faults. These responses are depicted in terms of terminal voltage (pu) and pitch angle (degrees) over a 10-second time interval. Terminal Voltage represents the per unit (pu) voltage at the terminals of the wind turbine. A value of 1 pu indicates the nominal voltage level. Pitch Angle indicates the angle of the wind turbine blades relative to the wind direction, measured in degrees. Adjustments in the pitch angle help in regulating the turbine's power output during disturbances. By conducting a thorough comprehensive analysis, the following observations have been depicted.

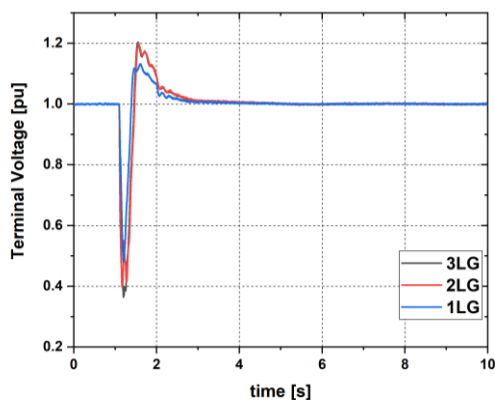


**Figure 13:** Variations in Terminal Voltage Across Different Fault Scenarios

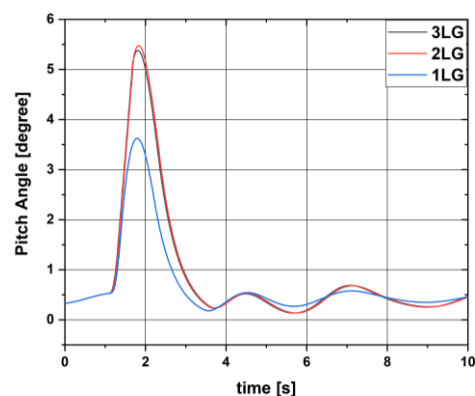


**Figure 14:** Variations in Pitch Angle Response Across Different Fault Scenarios

- **Initial Response (0 to 2 seconds):** All fault conditions lead to a significant drop in terminal voltage initially. The severity of the drop is most pronounced in the 3LG fault, followed by 2LG and 1LG faults. The pitch angle increases significantly for all fault conditions, with the 3LG fault showing the highest peak followed closely by the 2LG fault. The 1LG fault has a lower peak response.



- Recovery Phase (2 to 4 seconds):** The terminal voltage exhibits a transient recovery phase. In the case of the 3LG fault, the voltage overshoots above the nominal value before settling back, indicating a more severe transient disturbance. The 2LG and 1LG faults show similar behavior but with lesser overshoots and faster stabilization. The peak pitch angle is reached shortly after the fault occurs, with the 3LG fault peaking highest at around 5.5 degrees, followed by the 2LG fault, and then the 1LG fault peaking around 3.5 degrees. After reaching the peak, the pitch angle decreases as the system works to stabilize. The rate of decrease varies, with the 3LG and 2LG faults showing more pronounced oscillations compared to the 1LG fault.
- Steady State (after 4 seconds):** All fault conditions lead to the terminal voltage stabilizing back to the nominal value of 1 pu. The 1LG fault stabilizes the fastest, followed by 2LG and then 3LG faults. The pitch angles for all fault conditions converge towards a steady-state value, which is slightly above 1 degree for 3LG and 2LG faults, and just under 1 degree for the 1LG fault. Minor oscillations persist but gradually dampen out.

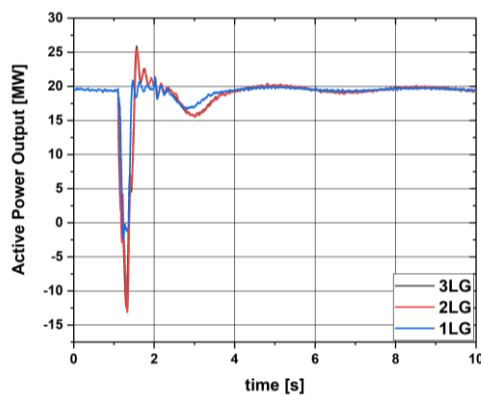


**Figure 15:** Variations in MW Output Response Across Different Fault Scenarios

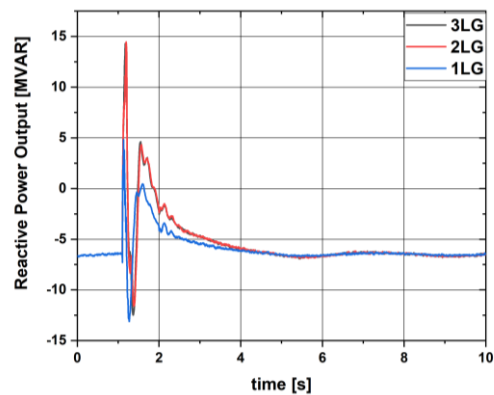


**Figure 16:** Variations in MVAR Reactive Power Output Response Across Different Fault Types

Figure 15 and Figure 16 depict the time response of a power system output to different types of faults. Specifically, represents the active and reactive power outputs of the system over a period of 10 seconds for three types of faults. Figure 15 represents the active power output in megawatts (MW), ranging from -14 MW to 26 MW. All fault types cause a significant disturbance in the active power output initially, as indicated by the sharp changes around the 1-second mark. The system stabilizes and returns to a steady state after approximately 4 to 5 seconds. The 3LG fault shows the most dramatic initial dip, while the 1LG fault shows a comparatively moderate disturbance. Figure 16 represents the reactive power output in megavolt-amperes reactive (MVAR), ranging from -14 MVAR to 14 MVAR. Similar to active power, all fault types cause a significant disturbance in reactive power output, with noticeable spikes around the 1-second mark. The system stabilizes and returns to a steady state after approximately 3 to 4 seconds. The 3LG fault causes the most significant spike and dip in reactive power, followed by the 2LG and 1LG faults respectively.

The system demonstrates the ability to recover from these disturbances, returning to near steady-state conditions. However, the recovery characteristics (i.e., overshoot and settling time) differ depending on the type of fault. Understanding these responses is crucial for designing and implementing protection schemes in power systems. It helps in setting appropriate protection settings for relays and circuit breakers, designing systems to withstand and quickly recover from faults and ensuring the reliability and stability of the power grid during and after fault conditions.

#### IV. CONCLUSION

The integration of renewable energy sources, particularly wind power, into the electrical grid presents substantial challenges in maintaining grid stability. This research focuses on enhancing the Low-Voltage Ride-Through (LVRT) capability of a Doubly-Fed Induction Generator (DFIG) wind turbine, a critical component for ensuring wind turbines remain operational during voltage dips or faults, thereby contributing to overall grid reliability. LVRT is pivotal in preventing widespread power outages and ensuring continuous power supply during disturbances. Grid codes, which stipulate specific requirements for voltage recovery post-fault,

underscore the necessity for robust LVRT capabilities. Non-compliance with these codes can result in the disconnection of wind turbines, exacerbating grid instability. To comprehensively evaluate the LVRT performance of the DFIG wind turbine system, both dynamic and transient analyses are indispensable. Dynamic analysis explores the system's behaviour over extended periods under fluctuating wind conditions, providing insights into long-term stability and performance. Conversely, the transient analysis focuses on short-duration events like faults, critical for understanding immediate system responses and resilience. This research is a vital contribution to the ongoing efforts to integrate wind energy into the power grid. By enhancing the LVRT capability of DFIG wind turbines, the study addresses a critical barrier to the widespread adoption of renewable energy sources. Ensuring grid stability amidst increasing renewable energy penetration is crucial for the transition to a sustainable energy future.

Achieving swift voltage recovery and optimal reactive power injection poses significant challenges. This paper aims to simulate and analyze the performance of the power system under various fault conditions, employing the PSCAD/EMTDC® simulation tool. The focus is on the effectiveness of finely tuned Proportional-Integral (PI) controllers in enhancing the LVRT capability of wind turbines, ensuring compliance with stringent grid codes and maintaining overall grid stability. The finely tuned PI controllers prove to be effective in managing voltage recovery and reactive power injection during fault conditions.

### **ACKNOWLEDGEMENTS**

The author extends sincere gratitude to Dr. Oihane Abarrategi, Professor, University of the Basque Country, Spain for her invaluable suggestions, support and feedback throughout this research work.

### **V. REFERENCES**

- [1] Prema HJ, Hazari MR, Mannan MA, Rahman MA. Design and Analysis of a Virtual Synchronous Generator Control Scheme to Augment FRT Capability of PMSG-Based Wind Turbine. *Adv Sci Technol Eng Syst J*. 2022 Dec;7(6):236-43.
- [2] Akanto JM, Islam MK, Jahan E, Hazari MR, Mannan MA, Rahman MA. Dynamic Analysis of Grid-connected Hybrid Wind Farm. *Int J Power Electron Drive Syst (IJPEDS)*. 2023 Jun;14(2):1230-7.
- [3] Singh AK, Agrawal S, Thakur A, Gupta M. Optimization of PI controllers using Elephant Herding Algorithm for voltage regulation in wind energy conversion systems. *IEEE Trans Power Electron*. 2019 Aug;34(8):7025-34.
- [4] Mandal JK, Roy P, Banerjee S. Enhanced LVRT capability using hybrid wind turbine technology and fuzzy logic control. *IEEE Trans Sustain Energy*. 2020 Jul;11(3):1627-36.
- [5] Hossain MA, Hossain TM, Al-Durra A. LVRT enhancement in PV systems using Salp Swarm Algorithm optimized controllers. *IEEE Access*. 2020;8:156374-84.
- [6] Zhang Y, Liu Y, Tang X. Hybrid CSO-GWO optimization for PI controller design in offshore wind farms. *IEEE Trans Ind Electron*. 2020 Sep;67(9):7890-9.
- [7] Gao L, Li M, Zhou H. Coordinated control strategy for LVRT and frequency stability using battery storage systems. *IEEE Trans Smart Grid*. 2021 Jan;12(1):345-54.
- [8] Babu PS, Ghosh K. Refining PI controllers using the Taguchi method for LVRT in wind energy systems. *IEEE Trans Ind Appl*. 2020 Nov-Dec;56(6):6354-62.
- [9] Alavi AH, Wang GG. Elephant Herding Optimization: Variants, Hybrids, and Applications. *Mathematics*. 2020;8(9):1415.
- [10] Hussain HA. Enhanced Control of Back-to-Back Converters in Wind Energy Conversion Systems Using Two-Degree-of-Freedom (2DOF) PI Controllers. *Electronics*. 2023;12(20):4221.
- [11] Ravi Kumar KS, Subburaj P. Salp Swarm Algorithm Based Maximum Power Point Tracking for PV Systems. *IEEE Access*. 2021;9:104337-45.
- [12] Saeedifard M, Gholamian SA, Ameli MT. A Coordinated Control Strategy for LVRT and Frequency Stability Improvement in Microgrids. *IEEE Trans Sustain Energy*. 2021;12(3):1543-54.
- [13] Choi H, Choi JH, Ahn JH. Performance Comparison of STATCOM and SVC in Improving Voltage Stability of Power Systems. *IEEE Trans Power Delivery*. 2021;36(4):2032-41.

- 
- [14] Patra TK, Panda RK, Mohanty A. Application of Taguchi Method in Optimization of PI Controller for DFIG Based Wind Energy System. IEEE Access. 2020;8:43234-43.
- [15] Bijoy HM, et al. Current Status and Challenges of Renewable Energy Implementation in Bangladesh. 2023 Innovations in Power and Advanced Computing Technologies (i-PACT), Kuala Lumpur, Malaysia. 2023. p. 1-7. doi: 10.1109/i-PACT58649.2023.10434878.
- [16] Mondol A, Hazari MR, Mannan MA, Tamura J. Hybrid Power System Frequency Control including Wind Farm using Battery Storage System. AIUB J Sci Eng (AJSE). 2020 Apr;19(1):41-6
- [17] Hazari MR, Mannan MA, Muyeen SM, Umemura A, Takahashi R, Tamura J. Transient stability augmentation of hybrid power system based on synthetic inertia control of DFIG. 2017 Australasian Universities Power Engineering Conference (AUPEC), Melbourne, VIC, Australia. 2017. p. 1-6. doi: 10.1109/AUPEC.2017.8282485.
- [18] Hosseinzadeh N, Aziz A, Mahmud A, Gargoom A, Rabbani M. Voltage Stability of Power Systems with Renewable-Energy Inverter-Based Generators: A Review. Electronics. 2021 Jan;10(2):115. doi:10.3390/electronics10020115.
- [19] Alam M, Abido M, Hussein A, El-Amin I. Fault Ride through Capability Augmentation of a DFIG-Based Wind Integrated VSC-HVDC System with Non-Superconducting Fault Current Limiter. Sustainability. 2019 Feb;11(5):1232. doi: 10.3390/su11051232.
- [20] Actual data of wind speed (Hokkaido Island), available at: [https://docs.google.com/spreadsheets/d/1-B4ykzxTe3qEyEuz47X0gqpi7B4\\_M4ja/edit?usp=sharing&oid=110918670424039267397&rtpof=true&s d=true](https://docs.google.com/spreadsheets/d/1-B4ykzxTe3qEyEuz47X0gqpi7B4_M4ja/edit?usp=sharing&oid=110918670424039267397&rtpof=true&s d=true) (accessed May 15, 2024).